



# Growth and characterization of organic material 3,4-dimethoxybenzaldehyde-2,4-dinitroaniline single crystal

R. P. Jebin<sup>1</sup>, T. Suthan<sup>2,\*</sup> , T. R. Anitha<sup>2</sup>, N. P. Rajesh<sup>3</sup>, and G. Vinita<sup>4</sup>

<sup>1</sup>Department of Physics, Noorul Islam Centre for Higher Education, Kumaracoil 629180, India

<sup>2</sup>Department of Physics, Lekshmipuram College of Arts and Science, Tamil Nadu, Neyyoor 629802, India

<sup>3</sup>Centre for Radiation Environmental Science and Technology, Sri Sivasubramaniya Nadar College of Engineering, Kalavakkam, Chennai 603110, India

<sup>4</sup>Division of Physics, VIT, Chennai 600175, India

**Received:** 26 October 2020

**Accepted:** 8 December 2020

**Published online:**

15 January 2021

© The Author(s), under exclusive licence to Springer Science+Business Media, LLC part of Springer Nature 2021

## ABSTRACT

The organic material 3,4-dimethoxybenzaldehyde-2,4-dinitroaniline was synthesised and the single crystal has been grown by slow evaporation technique. Single-crystal X-ray diffraction studies show that the grown 3,4-dimethoxybenzaldehyde-2,4-dinitroaniline single crystal belongs to the monoclinic system with the centrosymmetric space group  $P2_1/n$ . The FTIR and FT-Raman spectra were recorded to identify the functional groups present in the grown crystal. The optical property of the grown crystal was analyzed by UV–Vis–NIR studies and determines the optical band gap, the refractive index, the optical conductivity and the Urbach energy. The photoluminescence (PL) studies show that the grown crystal has green colour emission. The thermal property of the grown crystal was analysed by thermogravimetric (TG) and differential thermal analyses (DTA). The kinetic parameters such as the activation energy, frequency factor, entropy, enthalpy and Gibbs-free energy are computed from TGA data using Coats–Redfern method. The dielectric studies were analyzed by using the parallel plate capacitor method. The activation energy is calculated from Arrhenius plot. The electronic properties such as the plasma energy, the Penn gap, the Fermi energy and the electronic polarizability are calculated. The third order nonlinear optical properties of 3,4-dimethoxybenzaldehyde-2,4-dinitroaniline was measured by the Z-scan technique using 532 nm diode pumped continuous wave (CW) Nd:YAG laser.

Address correspondence to E-mail: suthantr@yahoo.co.in

## 1 Introduction

In the recent years, many innovative research reports have been focused on NLO materials due to its potential applications in modern optical data storage, frequency mixing, holographic imaging, telecommunication, integrated optics etc. Nonlinear optical materials have the ability to generate new electromagnetic fields with changed frequencies, phases and other physical properties. Nonlinear optics has come under the limelight of scientific research since the late 1960s with the onset of laser followed by the confirmation of harmonic generation in quartz. Nonlinear optics is the study of the interaction of light with matter when the response of a material system to an applied optical field depends in a nonlinear manner on the strength of the optical field. The synthesis of new and efficient frequency conversion materials has resulted in the development of novel organic materials.

Organic NLO materials offer a much larger versatility in assembling different crystal structures, enabling the fine tuning of the linear and nonlinear optical properties of the materials compared to inorganic materials. The advanced development in the crystal growth technology has exposed the attractive nonlinear optical properties of the crystals. This has enabled the commercial development of single crystals with promising nonlinear optical (NLO) properties [1–4]. Most of the optical fields researchers are also require a clear understanding of the third order nonlinear optical properties, which is an important part of these investigations. A vital goal for designing the molecules with large third-order nonlinearities has a feature devices used in the optical signal processing [5, 6]. To evaluate a material for the above application, its nonlinear refractive index and nonlinear absorption coefficient must be characterized. Several techniques are available for the measurement of nonlinear refraction in materials such as nonlinear interferometry, degenerate four-wave mixing, nearly degenerate three-wave mixing, ellipse rotation and beam-distortion measurements. Z-scan is a simple and popular experimental technique for the accurate measurements of intensity dependent nonlinear susceptibilities, nonlinear refractive index and nonlinear absorption coefficient [7–9].

The 3,4-dimethoxybenzaldehyde is a non-hygroscopic organic compound and its molecular formula is  $C_9H_{10}O_3$ . It can be used as an intermediate in the

synthesis of some pharmaceutical drugs. The 2,4-dinitroaniline is a non-hygroscopic organic compound and its molecular formula is  $C_6H_5N_3O_4$ . The dinitroanilines are intermediates in the preparation of various industrially important chemicals including dyes and pesticides. The organic material 3,4-dimethoxybenzaldehyde-2,4-dinitroaniline single crystal was successfully grown by slow evaporation technique using acetone as the solvent. The grown crystals were characterized by the single crystal X-ray diffraction, powder XRD, FTIR, FT-Raman, optical (UV–Vis–NIR), photoluminescence (PL), thermal (TG/DTA), dielectric measurements and the third-order nonlinear optical studies.

## 2 Experimental

The organic material 3,4-dimethoxybenzaldehyde-2,4-dinitroaniline was successfully synthesized using commercially available AR grade 3,4-dimethoxybenzaldehyde and 2,4-dinitroaniline chemicals in the equimolar ratio (1:1). The synthesized material was dissolved in acetone solvent. The solubility curve of 3,4-dimethoxybenzaldehyde-2,4-dinitroaniline at the various temperature ranges from 32 to 40 °C is shown in Fig. 1. The result shows that the solubility increases with the increase in temperature. The prepared solutions were then filtered and the purity of the materials was achieved by repetitive recrystallization process. For the crystal growth process the solvent was allowed to evaporate slowly at room

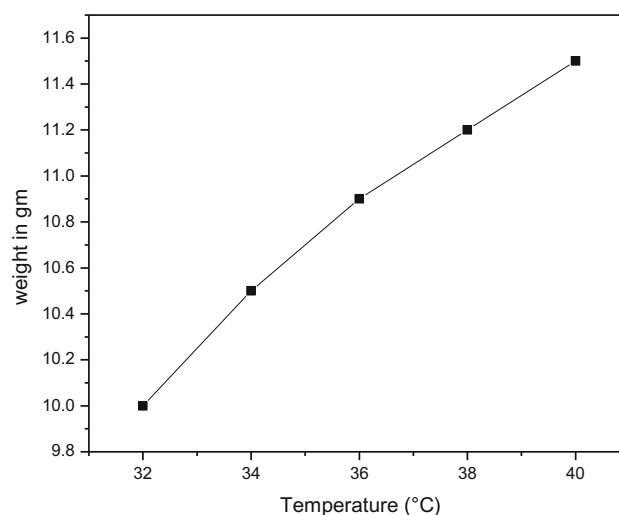


**Fig. 1** Solubility curve of 3,4-dimethoxybenzaldehyde-2,4-dinitroaniline

temperature. The good optical quality crystals were harvested within few days. The photograph of the grown 3,4-dimethoxybenzaldehyde-2,4-dinitroaniline single crystal is shown in Fig. 2.

### 3 Results and discussion

#### 3.1 Single-crystal XRD analysis

The Enraf Nonius CAD4MV31 single crystal X-ray diffractometer with the MoK $\alpha$  ( $\lambda = 0.717073 \text{ \AA}$ ) is used to estimate the structure and the crystallographic parameters of the grown 3,4-dimethoxybenzaldehyde-2,4-dinitroaniline single crystal. This technique is directly connected to a single crystal refinement module, where the data generated from the X-ray analysis is interpreted and refined to obtain the crystal structure. The structure was solved by direct methods using the 2772 reflections and the refinements were carried out by the full-matrix least-squares technique using SHELXL97 package. It is observed that the grown 3,4-dimethoxybenzaldehyde-2,4-dinitroaniline crystal belongs to monoclinic crystal system with the centrosymmetric space group  $P2_1/n$ . The structure and the lattice parameter values of 3,4-dimethoxybenzaldehyde-2,4-dinitroaniline single crystal are deposited in the Cambridge Crystallographic Data Centre (CCDC) [10]. The obtained cell parameters and the technical details of data acquisition and selected refinement results are listed in Table 1. The molecular structure and the crystallographic numbering scheme of 3,4-dimethoxybenzaldehyde-2,4-dinitroaniline crystal is shown in Fig. 3 and the Packing diagram of the grown crystal is shown in Fig. 4.

#### 3.2 Powder XRD studies

Powder X-ray diffraction pattern was recorded using a XPERT-PRO diffractometer with CuK $\alpha_1$  ( $\lambda = 1.54056 \text{ \AA}$ ) radiation. The diffraction was recorded over a range of 10 to 70° at the rate of 1° min<sup>-1</sup>. The recorded X-ray pattern of the 3,4-dimethoxybenzaldehyde-2,4-dinitroaniline is shown in Fig. 5. All the reflections are observed at room temperature. The obtained  $hkl$  planes are determined by using the two theta software. The determined sharp diffraction Bragg's peaks at the specific  $2\theta$  angle shows the grown 3,4-dimethoxybenzaldehyde-2,4-dinitroaniline crystals have the good crystalline quality.

#### 3.3 FTIR and FT-Raman spectral analyses

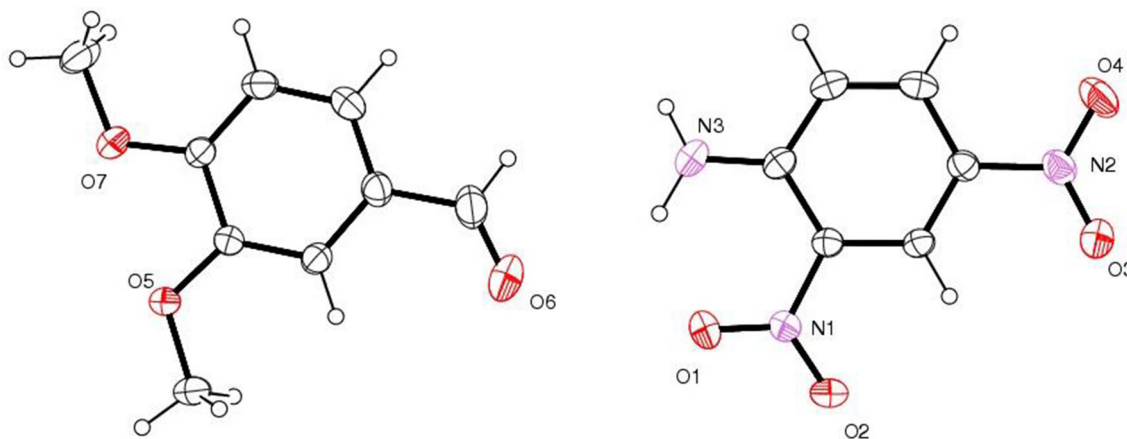
The functional groups of the grown 3,4-dimethoxybenzaldehyde-2,4-dinitroaniline crystal has been identified by FTIR and FT-Raman analyses. The FTIR spectrum was recorded using the Perkin-Elmer FTIR spectrum RIX spectrometer by the KBr pellet technique, with a limit of 4000–400 cm<sup>-1</sup>. The FT-Raman spectrum was recorded using the BRUKER-RFS27 FT-Raman spectrometer in the limit of 4000–50 cm<sup>-1</sup>. The FTIR spectrum of the grown crystal 3,4-dimethoxybenzaldehyde-2,4-dinitroaniline is shown in the Fig. 6 and the FT-Raman spectrum is shown in the Fig. 7. The absorption peaks observed in the IR and the Raman spectrum at 2845 cm<sup>-1</sup> and 2843 cm<sup>-1</sup> may be due to H-C=O stretching and it confirms the presence of aldehyde. The peaks in the IR spectrum at 1627 cm<sup>-1</sup> and in the Raman spectrum at 1620 cm<sup>-1</sup> is due to N-H bending. The absorption peak in the FTIR spectrum at 1675 cm<sup>-1</sup> and the peak in the Raman spectrum at 1674 cm<sup>-1</sup> were assigned as -C=C- stretching. The peaks observed almost nearly 1327 cm<sup>-1</sup> in FTIR and

**Fig. 2** Photograph of 3,4-dimethoxybenzaldehyde-2,4-dinitroaniline



**Table 1** 3,4-dimethoxybenzaldehyde-2,4-dinitroaniline single XRD crystal data and structure refinement parameters

Chemical formula	$C_{15}H_{15}N_3O_7$
Formula weight	349.30 g/mol
Temperature	296(2) K
Wavelength	0.71073 Å
Crystal size	0.100 × 0.220 × 0.250 mm
Crystal system	Monoclinic
Space group	$P2_1/n$
Unit cell dimensions	$a = 11.1220(4)$ Å, $\alpha = 90^\circ$ $b = 12.3161(4)$ Å, $\beta = 105.4969(18)^\circ$ $c = 11.9076(4)$ Å, $\gamma = 90^\circ$
Volume	1571.80(9) Å <sup>3</sup>
Z	4
Density (calculated)	1.476 g/cm <sup>3</sup>
Absorption coefficient	0.119 mm <sup>-1</sup>
$F(000)$	728
Theta range for data collection	2.23 to 25.00°
Index ranges	$-12 \leq h \leq 13$ , $-13 \leq k \leq 14$ , $-14 \leq l \leq 10$
Reflections collected	11,570
Independent reflections	2772 [ $R(\text{int}) = 0.0196$ ]
Coverage of independent reflections	100.0%
Absorption correction	Multi-scan
Max. and min. transmission	0.9880 and 0.9710
Refinement method	Full-matrix least-squares on $F^2$
Refinement program	SHELXL-2014/7 (Sheldrick, 2014)
Function minimized	$\Sigma w(F_o^2 - F_c^2)^2$
Data/restraints/parameters	2772/0/237
Goodness-of-fit on $F^2$	1.050
$\Delta/\sigma_{\text{max}}$	0.001
Final $R$ indices 2224 data; $I > 2\sigma(I)$	$R1 = 0.0351$ , $wR2 = 0.1198$
All data	$R1 = 0.0460$ , $wR2 = 0.1356$
Weighting scheme	$w = 1/[\sigma^2(F_o^2) + (0.1000P)^2 + 0.0002P]$ , where $P = (F_o^2 + 2F_c^2)/3$
Extinction coefficient	0.0060(20)
Largest diff. peak and hole	0.143 and $-0.158$ eÅ <sup>-3</sup>
R.M.S. deviation from mean	0.033 eÅ <sup>-3</sup>

**Fig. 3** Crystallographic numbering scheme of 3,4-dimethoxybenzaldehyde-2,4-dinitroaniline crystal

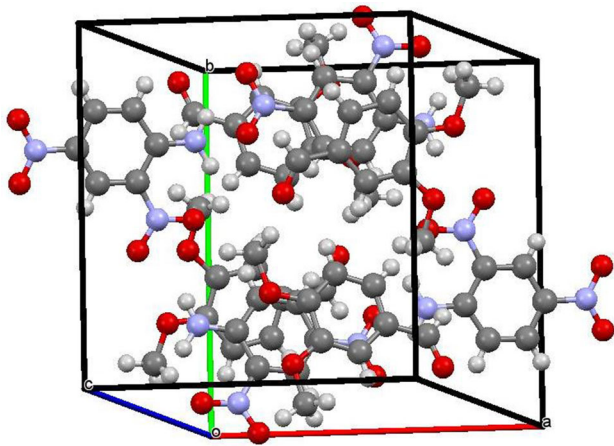


**Fig. 4** Packing diagram of 3,4-dimethoxybenzaldehyde-2,4-dinitroaniline crystal

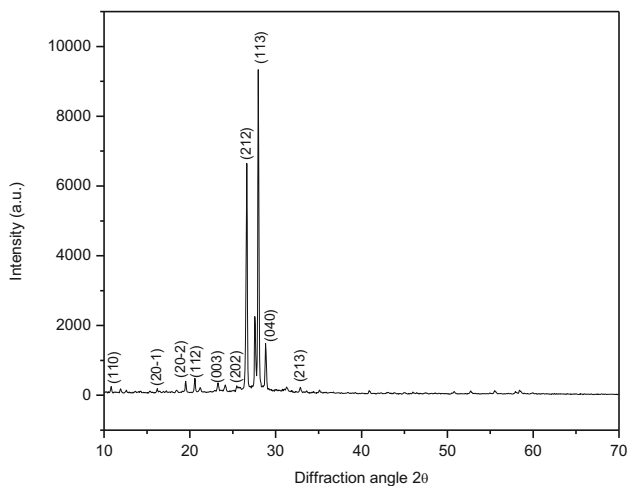


**Fig. 5** Powder XRD pattern of 3,4-dimethoxybenzaldehyde-2,4-dinitroaniline

around  $1328\text{ cm}^{-1}$  in Raman have been assigned as the C–N stretching. The absorption peaks at  $1497\text{ cm}^{-1}$  and  $1518\text{ cm}^{-1}$  in FTIR and Raman spectra have been assigned as the N–O asymmetric stretching and it shows the presence of nitro compounds. The absorption peak at  $922\text{ cm}^{-1}$  in FTIR spectrum and the absorption peak at  $924\text{ cm}^{-1}$  in Raman spectrum is due to O–H bending.

### 3.4 UV–Vis–NIR studies

The optical transmittance plays a vital role in identifying a potential NLO material because a material can have applicability only if it has a wide optical transparent window without absorption [11]. Hence it is important to study the transmission of

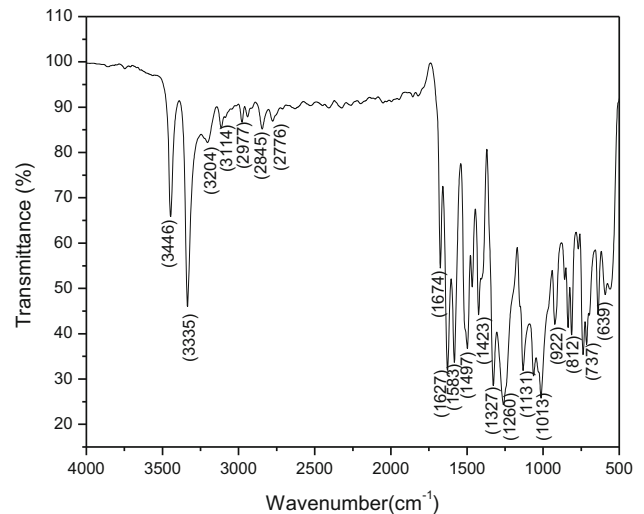


**Fig. 6** FTIR spectrum of 3,4-dimethoxybenzaldehyde-2,4-dinitroaniline

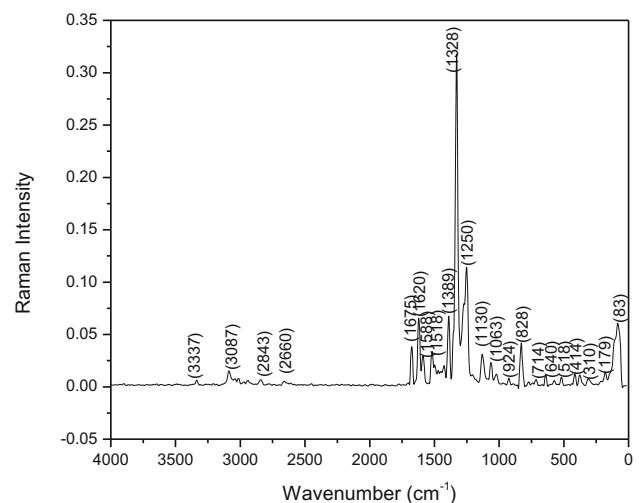


**Fig. 7** FT-Raman spectrum of 3,4-dimethoxybenzaldehyde-2,4-dinitroaniline

electromagnetic waves of the UV–Vis–NIR range through the NLO material. The transmission spectrum was recorded using a Perkin-Elmer Lambda 35 UV–Vis–spectrophotometer in the range 190–1100 nm. The transparent single crystal of thickness 2 mm was used for the analysis and the recorded transmittance spectrum is shown in Fig. 8a. The obtained result shows that the grown 3,4-dimethoxybenzaldehyde-2,4-dinitroaniline single crystal has nearly 80% transparency. The electronic transition  $\sigma \rightarrow \sigma^*$  fall into the far-ultraviolet region;  $\pi \rightarrow \pi^*$  and  $n \rightarrow \sigma^*$  transitions appear near the border line of the near-ultraviolet and far-ultraviolet

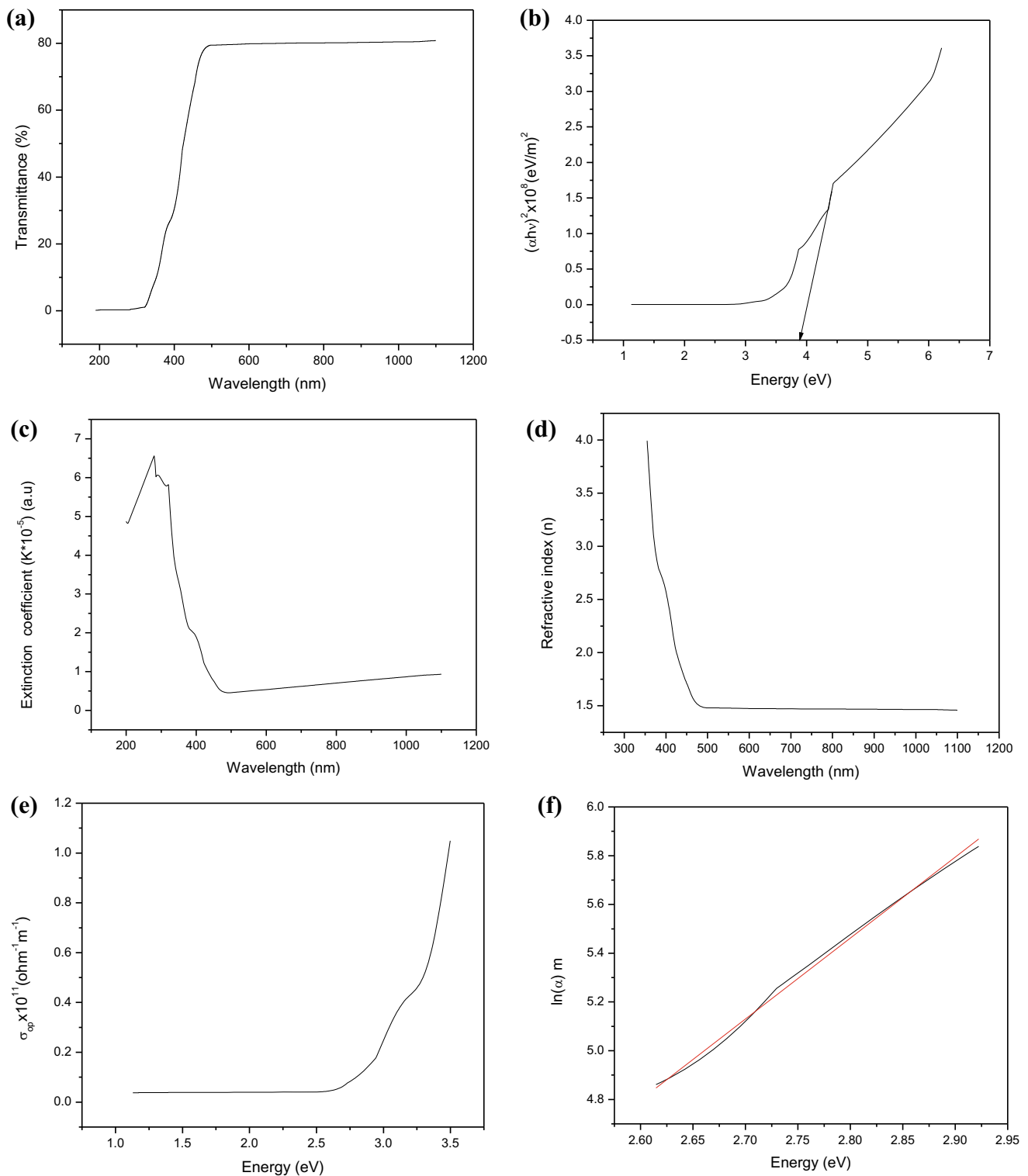


**Fig. 8** **a** UV-Vis-NIR spectrum of 3,4-dimethoxybenzaldehyde-2,4-dinitroaniline. **b** Tauc plot of  $(\alpha h\nu)^2$  versus energy for grown 3,4-dimethoxybenzaldehyde-2,4-dinitroaniline. **c** Plot of extinction coefficient versus wavelength for 3,4-dimethoxybenzaldehyde-2,4-dinitroaniline crystal. **d** Plot of refractive index versus wavelength

for 3,4-dimethoxybenzaldehyde-2,4-dinitroaniline crystal. **e** Optical conductivity as a function of photon energy for grown 3,4-dimethoxybenzaldehyde-2,4-dinitroaniline. **f** Plot of  $\ln(\alpha)$  versus photon energy for grown 3,4-dimethoxybenzaldehyde-2,4-dinitroaniline

regions; and  $n \rightarrow \pi^*$  transition fall into the near-ultraviolet and visible regions [12]. The cut-off wavelength of the crystal is observed around 315 nm which is due to  $n \rightarrow \pi^*$  transition in the compound. The crystal has good transmittance in the entire visible and the near infrared regions. The wide transmittance range and the lower cut-off region will be helpful for these crystals for NLO applications.

The measured transmittance ( $T$ ) was used to calculate the absorption coefficient ( $\alpha$ ) using the formula

$$\alpha = \frac{2.3026 \log(1/T)}{t}$$

where  $t$  is the thickness of the sample. The optical band gap ( $E_g$ ) was calculated using the Tauc relation

$$h\nu\alpha = A(h\nu - E_g)^m$$

where  $A$  is a constant,  $E_g$  is the optical band gap,  $h$  is the Planck's constant,  $\nu$  is the frequency of the incident photons and  $m$  is the index, which can have different values (2, 3, 1/2 and 3/2) corresponding to indirect allowed, indirect forbidden, direct allowed and direct forbidden transitions respectively [13, 14]. The band gap of 3,4-dimethoxybenzaldehyde-2,4-dinitroaniline crystal was estimated by plotting  $(\alpha h\nu)^2$  versus  $h\nu$  as shown in Fig. 8b and extrapolating the linear portion near the onset of absorption edge to the X-axis. From the figure, the value of optical band gap is found to be 3.9 eV.

The optical behaviour of materials is important to determine their usage in optoelectronic devices. The study of optical constants of a material such as refractive index and extinction coefficient is quite essential to examine the material's potential optoelectronic applications. The extinction coefficient ( $K$ ) can be obtained from the equation

$$K = \frac{\lambda\alpha}{4\pi}$$

Figure 8c shows the variation of extinction coefficient ( $K$ ) with wavelength. The transmittance ( $T$ ) is given by

$$T = \frac{(1 - R)^2 \exp(-\alpha t)}{1 - R^2 \exp(-2\alpha t)}$$

The reflectance ( $R$ ) in terms of the absorption coefficient can be obtained from the above equation

$$R = \frac{\exp(-\alpha t) \pm \sqrt{\exp(-\alpha t)T - \exp(-3\alpha t)T + \exp(-2\alpha t)T^2}}{\exp(-\alpha t) + \exp(-2\alpha t)T}$$

The refractive index ( $n$ ) can be determined from reflectance data using the equation

$$n = \frac{-(R + 1) \pm 2\sqrt{R}}{(R - 1)}$$

The variation of refractive index with wavelength for 3,4-dimethoxybenzaldehyde-2,4-dinitroaniline single crystal is shown in Fig. 8d. The optical conductivity ( $\sigma_{op}$ ) is a measure of the frequency response of the material when it is irradiated with light.

$$\sigma_{op} = \frac{\alpha mc}{4\pi}$$

where  $c$  is the velocity of light. The energy dependence of optical conductivity of the grown crystal is shown in Fig. 8e. It can be seen clearly from the figure that the optical conductivity increases abruptly after 2.75 eV for the grown crystal.

Urbach energy ( $E_U$ ) characterizes the amount of the absorption edge smearing due to the lattice disorder and non-stoichiometry showing the imperfections in crystalline nature. An exponential part called Urbach tail is found along the absorption coefficient curve near the optical band edge [15]. This exponential tail appears to be more for poor crystalline materials and amorphous materials. If this tail appears to be a minimum, this indicates the good crystalline nature and the perfection in lattice sites. The relationship between absorption coefficient  $\alpha$  and energy of photons ( $h\nu$ ) near the optical band gap edge is known as Urbach empirical rule, which is given by the following exponential equation

$$\alpha = \alpha_0 \exp\left(\frac{h\nu}{E_U}\right)$$

where  $\alpha_0$  is a constant and  $E_U$  denotes the Urbach energy. Taking logarithm on both sides of the above equation, one can get an equation of straight line and it is given as follows

$$\ln(\alpha) = \ln(\alpha_0) + \left(\frac{h\nu}{E_U}\right)$$

The Urbach energy ( $E_U$ ) can be obtained from the reciprocal of the slope of the straight line obtained by plotting  $\ln(\alpha)$  against the incident photon energy ( $h\nu$ ) which is shown in Fig. 8f. The value of  $E_U$  is found to be 0.3 eV which indicates the good crystallinity of the

grown crystal and less disorder near the optical band edge. Another relation correlating absorption coefficient  $\alpha$  and the optical band gap energy  $E_g$  suggested by Urbach is given below.

$$\alpha = \beta \exp \left[ \frac{\sigma(h\nu - E_0)}{K_B T} \right]$$

where  $\beta$  is the pre-exponential constant,  $\sigma$  is the steepness parameter and  $E_0$  is the transition energy which is equal to  $E_g$  for direct allowed transition. The above equation can be rewritten in the following form:

$$\ln(\alpha) = \left( \ln(\beta) - \frac{\sigma E_g}{K_B T} \right) + \left( \frac{\sigma(h\nu)}{K_B T} \right)$$

Comparing the equations of  $\ln(\alpha)$ , we get

$$\left( \frac{h\nu}{E_U} \right) = \left( \frac{\sigma(h\nu)}{K_B T} \right)$$

where  $K_B$  is the Boltzmann constant in eV/K and  $T$  is the absolute temperature. The steepness parameter  $\sigma$  can be calculated using the relation

$$\sigma = \left( \frac{K_B T}{E_U} \right)$$

The steepness parameter  $\sigma$  is found to be 0.078 which is used for evaluating the strength of the electron–phonon interaction by the relation

$$E_{e-p} = \frac{2}{3\sigma}$$

The various linear optical parameters of 3,4-dimethoxybenzaldehyde-2,4-dinitroaniline crystal are listed in Table 2.

### 3.5 Photoluminescence studies

In recent years, the efficient organic luminescent nonlinear optical (NLO) materials have attracted

**Table 2** Linear optical parameters of 3,4-dimethoxybenzaldehyde-2,4-dinitroaniline crystal

Parameters	Calculated values
Optical band gap ( $E_g$ )	3.9 eV
Urbach energy ( $E_U$ )	0.3 eV
The constant ( $\alpha_0$ )	0.022 m <sup>-1</sup>
Steepness parameter ( $\alpha$ )	0.078
Electron–phonon interaction ( $E_{e-p}$ )	8.53

worldwide tremendous research interests in the field of opto-electric devices. The organic benzaldehyde derivatives single crystals have obtained good photoluminescence properties [16–19]. The photoluminescence (PL) spectrum of the grown 3,4-dimethoxybenzaldehyde-2,4-dinitroaniline single crystal has been recorded by using the spectrofluorometer with the 450 W as high pressure Xenon lamp as the excitation source. The photoluminescence emission spectrum for the grown 3,4-dimethoxybenzaldehyde-2,4-dinitroaniline single crystal was shown in Fig. 9. The emission band was observed in the wave length range from 300 to 700 nm. The high intensity sharp peak was observed at 530 nm. The obtained results indicate that the grown, 3,4-dimethoxybenzaldehyde-2,4-dinitroaniline single crystal may have green emission.

### 3.6 Thermal analyses

The TG and DTA analyses are of massive importance as far as fabrication technology is concerned, as they provide the thermal stability of the material for fabrication, where a considerable amount of heat is generated during the cutting process. Thermal analysis was performed on the grown crystals to study the thermal stability and the melting point. The thermal behavior of the grown 3,4-dimethoxybenzaldehyde-2,4-dinitroaniline crystal was carried out by the thermogravimetric (TG) and the differential thermal analyses (DTA) using SDT Q600 V20.9

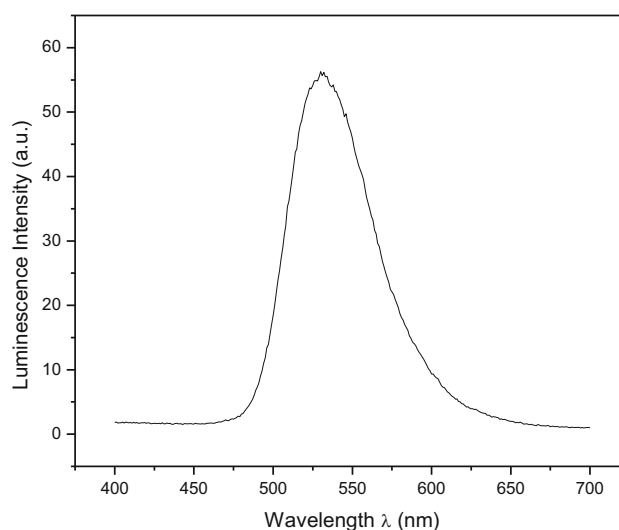


**Fig. 9** PL emission spectrum of 3,4-dimethoxybenzaldehyde-2,4-dinitroaniline



Build20 instrument, and the temperature ranges from 35 to 500 °C in the nitrogen atmosphere at a heating rate of 10 °C/min is being noted. The results obtained from the TG and the DTA are shown in Fig. 10a. The thermogravimetric analysis shows that the material is stable up to 137 °C. The first sharp endothermic curve in DTA is observed around 90 °C which indicates the melting point of the grown crystal. The second sharp endothermic peak is observed around 279 °C which is assigned as the decomposition point. From the TG/DTA analyses, it is observed that the grown 3,4-dimethoxybenzaldehyde-2,4-dinitroaniline single crystal have no phase transition or decomposition up to the melting point. The sharpness of the endothermic peaks observed in DTA indicates good degree of crystallinity of the sample.

TGA data can be used to study the kinetic parameters of thermal decomposition reaction such

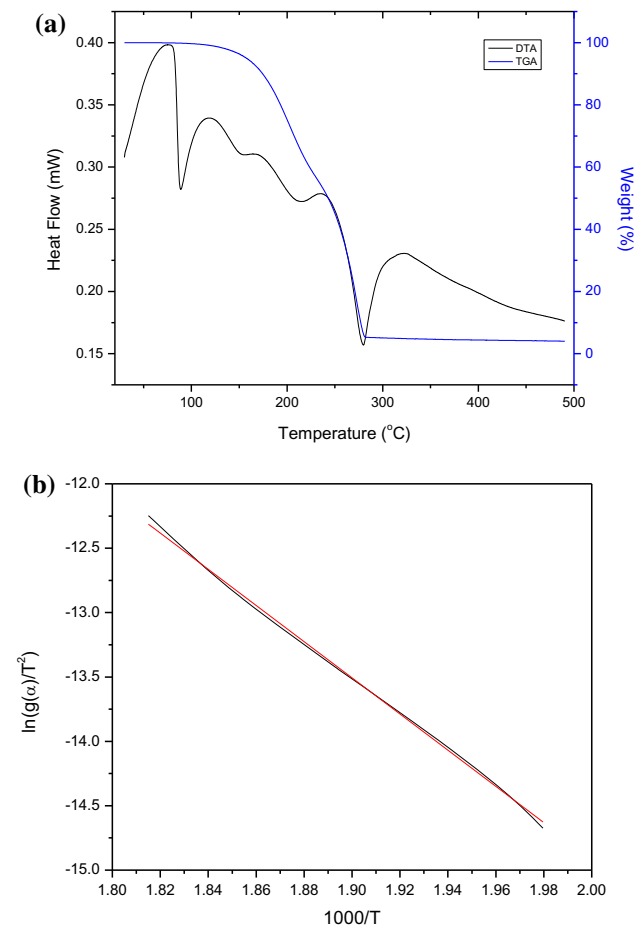


**Fig. 10** **a** TG/DTA spectrum of 3,4-dimethoxybenzaldehyde-2,4-dinitroaniline. **b** Coats-Redfern plot of 3,4-dimethoxybenzaldehyde-2,4-dinitroaniline crystal

as activation energy, frequency factor and order of reaction. Several methods have been reported for calculating the kinetic parameters of solid state reactions. In the present investigation, Coats-Redfern method is used for the evaluation of kinetic parameters from non-isothermal TG data at a constant heating rate [20–23]. The following equations are used for the kinetic analysis.

$$\begin{aligned} \ln \frac{g(\alpha)}{T^2} &= \ln \left[ \frac{-\ln(1-\alpha)}{T^2} \right] \\ &= \ln \left[ \left( \frac{AR}{\beta E_a} \right) \left( 1 - \frac{2RT}{E_a} \right) \right] - \frac{E_a}{RT} \quad (n = 1) \end{aligned}$$

$$\begin{aligned} \ln \frac{g(\alpha)}{T^2} &= \ln \left[ \left( \frac{1 - (1-\alpha)^{1-n}}{T^2(1-n)} \right) \right] \\ &= \ln \left[ \left( \frac{AR}{\beta E_a} \right) \left( 1 - \frac{2RT}{E_a} \right) \right] - \frac{E_a}{RT} \quad (n \neq 1) \end{aligned}$$

Since the term  $(2RT/E_a) \ll 1$ , the above equations can be rewritten as

$$\ln \frac{g(\alpha)}{T^2} = \ln \left[ \frac{-\ln(1-\alpha)}{T^2} \right] = \ln \left( \frac{AR}{\beta E_a} \right) - \frac{E_a}{RT} \quad (n = 1)$$

$$\ln \frac{g(\alpha)}{T^2} = \ln \left[ \left( \frac{1 - (1-\alpha)^{1-n}}{T^2(1-n)} \right) \right] = \ln \left( \frac{AR}{\beta E_a} \right) - \frac{E_a}{RT} \quad (n \neq 1)$$

where  $\alpha$  is the fraction of conversion;  $n$  is the order of the reaction;  $A$  is the frequency factor;  $E_a$  is the activation energy of the reaction;  $R$  is the gas constant;  $\beta$  is the heating rate and  $T$  is the absolute temperature. The value of fraction of conversion,  $\alpha$  was estimated by the relation

$$\alpha = \frac{W_0 - W}{W_0 - W_f}$$

where  $W_0$  is the initial weight;  $W$  is the instantaneous weight depending on time and temperature and  $W_f$  is the final weight of the sample. The plot of  $\ln \left[ \frac{g(\alpha)}{T^2} \right]$  versus  $\frac{1000}{T}$  is drawn for different values of  $n$ . Figure 10b shows the best linear fitted plot for  $n = 0.5$  which has been chosen as the order of reaction for the determination of the kinetic parameters. The slope of the straight line is used to calculate the activation energy,  $E_a$  and the intercept is used to calculate the frequency factor,  $A$ .

The thermodynamic parameters of 3,4-dimethoxybenzaldehyde-2,4-dinitroaniline crystal such as entropy of activation ( $\Delta S^*$ ), enthalpy of activation

( $\Delta H^*$ ) and Gibbs-free energy ( $\Delta G^*$ ) were calculated using the equations:

$$A = \left(\frac{KT_m}{h}\right) \exp\left(\frac{\Delta S^*}{R}\right)$$

$$\Delta H^* = E^* - RT$$

$$\Delta G^* = \Delta H^* - T\Delta S^*$$

where  $K$  is the Boltzmann constant;  $h$  is the Planck's constant and  $T_m$  is the maximum decomposition temperature. The calculated activation energy, frequency factor and other thermodynamic parameters are listed in Table 3. The negative value of the entropy of activation indicates that the activated complex is more ordered than the reactant and the decomposition reaction is slow. The change in Gibbs free energy  $\Delta G^*$  is the criterion that is used to indicate whether a chemical reaction is spontaneous or not. The positive value of  $\Delta G^*$  indicates that the decomposition of the grown crystal is non-spontaneous. The positive value of  $\Delta H^*$  indicates that the reaction is endothermic in nature and enhanced by the increase in temperature [24].

### 3.7 Dielectric properties

The dielectric analysis is an important tool that provides valuable information on the electrical properties of the material medium as a function of temperature and frequency. Dielectric properties are correlated with electro-optic properties of the crystals. The dielectric analysis for the grown 3,4-dimethoxybenzaldehyde-2,4-dinitroaniline crystal was carried out by the Agilent 4284A LCR Meter using the conventional parallel plate capacitor method [25, 26]. The capacitance and dielectric loss ( $\tan\delta$ ) were measured at various temperatures ranging from 308 to 373 K for five different frequencies 800 Hz, 1 kHz, 10 kHz, 100 kHz and 200 kHz. The

**Table 3** Kinetic parameters of 3,4-dimethoxybenzaldehyde-2,4-dinitroaniline crystal

Kinetic parameters	Calculated Values
Activation energy ( $E_a$ )	116.82 kJ mol <sup>-1</sup>
Frequency factor ( $A$ )	$3.55 \times 10^{10}$ s <sup>-1</sup>
Entropy of activation ( $\Delta S^*$ )	- 47.9 J K <sup>-1</sup> mol <sup>-1</sup>
Enthalpy of activation ( $\Delta H^*$ )	112.31 kJ mol <sup>-1</sup>
Gibbs free energy ( $\Delta G^*$ )	138.22 kJ mol <sup>-1</sup>

dielectric constant of the crystal was calculated using the relation

$$\epsilon_r = \left(\frac{1}{C_{air}}\right) \left(C_{crys} - C_{air} \left(1 - \frac{A_{crys}}{A_{air}}\right)\right) \left(\frac{A_{air}}{A_{crys}}\right)$$

where  $A_{crys}$  is the area of crystal touching the electrode and  $A_{air}$  is the area of electrode. The ac electrical conductivity  $\sigma_{ac}$  was calculated using the relation

$$\sigma_{ac} = \epsilon_0 \epsilon_r \omega \tan\delta$$

where  $\epsilon_0$  is the permittivity of free space,  $\omega$  is the angular frequency ( $\omega = 2\pi f$ , where  $f$  is the ac frequency considered) and  $\tan\delta$  is the dielectric loss factor. Figure 11a–c shows the dielectric constant ( $\epsilon_r$ ), dielectric loss ( $\tan\delta$ ) and ac conductivity ( $\sigma_{ac}$ ) evaluated for the grown single crystal at different temperatures and frequencies. It was observed that the dielectric constant is gradually increased with increase in temperature. This indicates the presence of space charge effects in addition to the electronic and the atomic conduction in the samples. The values of the dielectric constant and the dielectric loss decrease with the increase in frequency while the ac conductivity value increases with the increase in frequency. The high value of dielectric constant at low frequency is due to the contribution of all the polarization mechanisms namely electronic, ionic, orientation and space charge polarization. At high frequencies, the dielectric constant value decreases due to the absence of space charge polarization near the grain boundary interface. The low dielectric loss with high frequency implies that the grown 3,4-dimethoxybenzaldehyde-2,4-dinitroaniline single crystal possess enhanced optical quality with minimum defects and this parameter play a vital role for the construction of devices from nonlinear optical materials [27–29].

The activation energy in terms of electrical performance for 3,4-dimethoxybenzaldehyde-2,4-dinitroaniline single crystal was evaluated from Arrhenius plot using the relation [30]

$$\sigma_{ac} = \sigma_0 \exp\left(\frac{-E_a}{kT}\right)$$

where  $\sigma_{ac}$  is the electrical conductivity at temperature  $T$ ,  $\sigma_0$  is the pre-exponential factor,  $E_a$  is the activation energy,  $T$  is the absolute temperature and  $k$  is the Boltzmann constant. The activation energy can be calculated by using the slope of the Arrhenius plot of

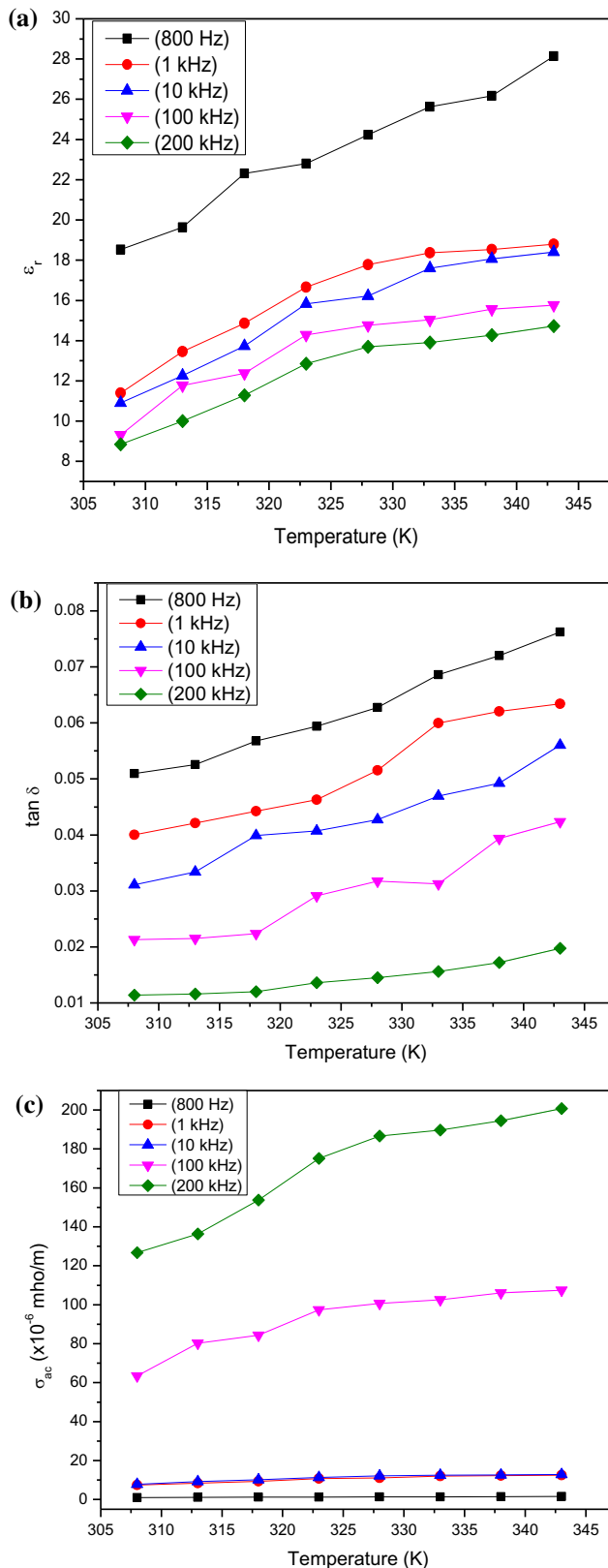


**Fig. 11** a Dielectric constants observed for 3,4-dimethoxybenzaldehyde-2,4-dinitroaniline. b Dielectric loss factors observed for 3,4-dimethoxybenzaldehyde-2,4-dinitroaniline. c AC electrical conductivities ( $\times 10^{-8}$  mho/m) observed for 3,4-dimethoxybenzaldehyde-2,4-dinitroaniline

$\ln(\sigma_{ac})$  versus  $\frac{1}{T}$ . ( $-E_a/k$ ) is the slope and the above equation can be written as

$$\ln \sigma_{ac} = \ln \sigma_0 + \text{slope} \left( \frac{1}{T} \right)$$

The value of slope can be computed from the linear graph of  $\ln(\sigma_{ac})$  versus  $\frac{1}{T}$  and the activation energy is now calculated as

$$E_a = -k \times \text{slope}$$

The variation of  $\ln \sigma_{ac}$  with  $1000/T$  for the frequency of 1 kHz is shown in Fig. 12 and the value of  $E_a$  is found to be 0.139 eV.

The dielectric permittivity and dielectric loss are dependent on the Penn gap, plasma energy, Fermi energy and the valence electron of compound [31]. The valence electron plasma energy ( $\hbar\omega_p$ ) is calculated using the relation

$$\hbar\omega_p = 28.8 \left( \frac{Z\rho}{M} \right)^{1/2}$$

where  $Z = (15 \times Z_C) + (15 \times Z_H) + (7 \times Z_O) + (3 \times Z_N) = 132$  is the total number of valence electrons. The density ( $\rho$ ) and molecular weight ( $M$ ) of 3,4-

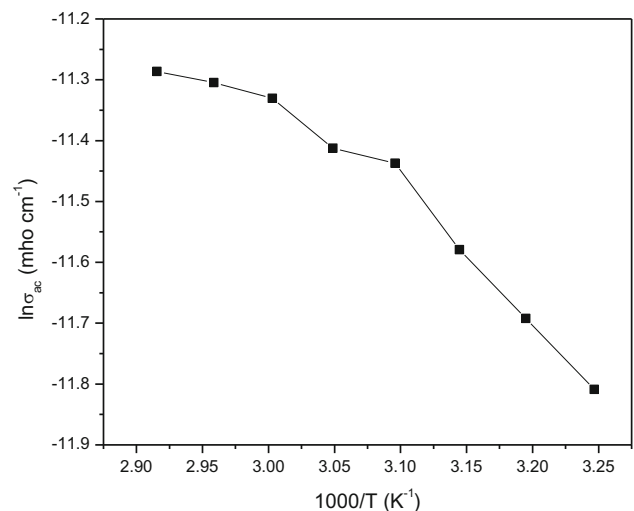


**Fig. 12** Arrhenius plot of  $\ln \sigma_{ac}$  versus  $1000/T$  for grown 3,4-dimethoxybenzaldehyde-2,4-dinitroaniline

dimethoxybenzaldehyde-2,4-dinitro aniline are 1.476 g/cm<sup>3</sup> and 349.3 g/mol, respectively. The Penn gap is calculated by fitting the dielectric constant with the Plasmon energy. The Penn gap,  $E_p$  and the Fermi energy,  $E_F$  in eV are given by the following relations

$$E_p = \frac{\hbar\omega_p}{(\epsilon_r - 1)^{1/2}}$$

$$E_F = 0.2948(\hbar\omega_p)^{4/3}$$

where  $\epsilon_r$  is the dielectric permittivity of the material at high frequency (1 kHz in the present case).

The electronic polarizability ( $\alpha$ ) of 3,4-dimethoxybenzaldehyde-2,4-dinitroaniline crystal is calculated,

- (a) Using the valence electron plasma energy relation

$$\alpha = \left( \frac{(\hbar\omega_p)^2 S_0}{(\hbar\omega_p)^2 S_0 + 3E_p^2} \right) \times \frac{M}{\rho} \times 0.396 \times 10^{-24} \text{ cm}^3$$

where ( $S_0$ ) is a constant which given as

$$S_0 = 1 - \left( \frac{E_p}{4E_F} \right) + \frac{1}{3} \left( \frac{E_p}{4E_F} \right)^2$$

- (b) (b) Using the Clausius–Mossotti relation

$$\alpha = \left( \frac{3M}{4\pi N_a \rho} \right) \left( \frac{\epsilon_r - 1}{\epsilon_r + 2} \right)$$

where  $N_a$  is Avogadro number ( $N_a = 6.023 \times 10^{23}$ ). The calculated electronic properties like plasma energy, Penn gap, Fermi energy and electronic polarizability obtained using valence electron plasma energy and Clausius–Mossotti relation for the 3,4-dimethoxybenzaldehyde-2,4-dinitroaniline crystal is listed in Table 4.

**Table 4** Electronic parameters of 3,4-dimethoxybenzaldehyde-2,4-dinitroaniline single crystal

Parameters	Calculated values
Plasma energy ( $\hbar\omega_p$ )	21.509 eV
Penn gap ( $E_p$ )	6.669 eV
Fermi energy ( $E_F$ )	17.634 eV
Electronic polarizability, ( $\alpha$ )	
From Penn analysis	$7.113 \times 10^{-23} \text{ cm}^3$
From Clausius–Mossotti relation	$7.284 \times 10^{-23} \text{ cm}^3$

### 3.8 Nonlinear optical studies

Z-scan technique is a well known technique for the measurement of optical nonlinearities of the materials, especially nonlinear refraction and nonlinear absorption. This method facilitates the simultaneous measurement of magnitude as well as sign of the nonlinear refractive index and nonlinear absorption coefficient of the material using open, closed and ratio of the closed-to open configurations of Z-scan. The position vector  $z$  of the sample is varied with respect to the focal plane of the lens and hence this technique is called Z-scan. In the present investigation, Z-scan experiment was performed using a 50 mW 532 nm diode pumped CW Nd:YAG Laser which was focused by a lens of focal length 3.5 cm. The intensity of laser output was 4.38 kW/cm<sup>2</sup>.

The laser beam waist ( $\omega_0$ ) at the focus is measured to be 15.84  $\mu\text{m}$ . The corresponding Rayleigh length  $z_0$  is calculated using the relation

$$z_0 = \frac{\pi\omega_0^2}{\lambda}$$

where  $\lambda$  is the laser wavelength. The value of  $z_0$  is calculated to be 1.48 mm. The optical cell of 1 mm width containing 3,4-dimethoxybenzaldehyde-2,4-dinitroaniline solution satisfied the thin sample condition  $L \ll z_0$  is translated across the focal region along the direction of the propagation laser beam. The transmission of the laser beam through the aperture placed in the far field was measured by using photo detector which is fed to the digital power meter. In the open aperture Z-scan mode, the aperture is replaced by a lens to collect the laser beam transmitted through the sample.

Figure 13a–c shows the closed, the open and the ratio of the closed to open normalized Z-scan of the 3,4-dimethoxybenzaldehyde-2,4-dinitroaniline sample in acetone at 60% transmittance. The peak followed by a valley normalized transmittance obtained from the closed aperture Z-scan data indicate that the signs of the refraction nonlinearity is negative, i.e., self-defocusing. The self-defocusing effect is due to the local variation in the refractive index with the temperature [32–34].

The difference between the normalized peak and valley transmittances,  $\Delta T_{p-v}$  can be evaluated from the closed aperture normalized transmittance data by the relation

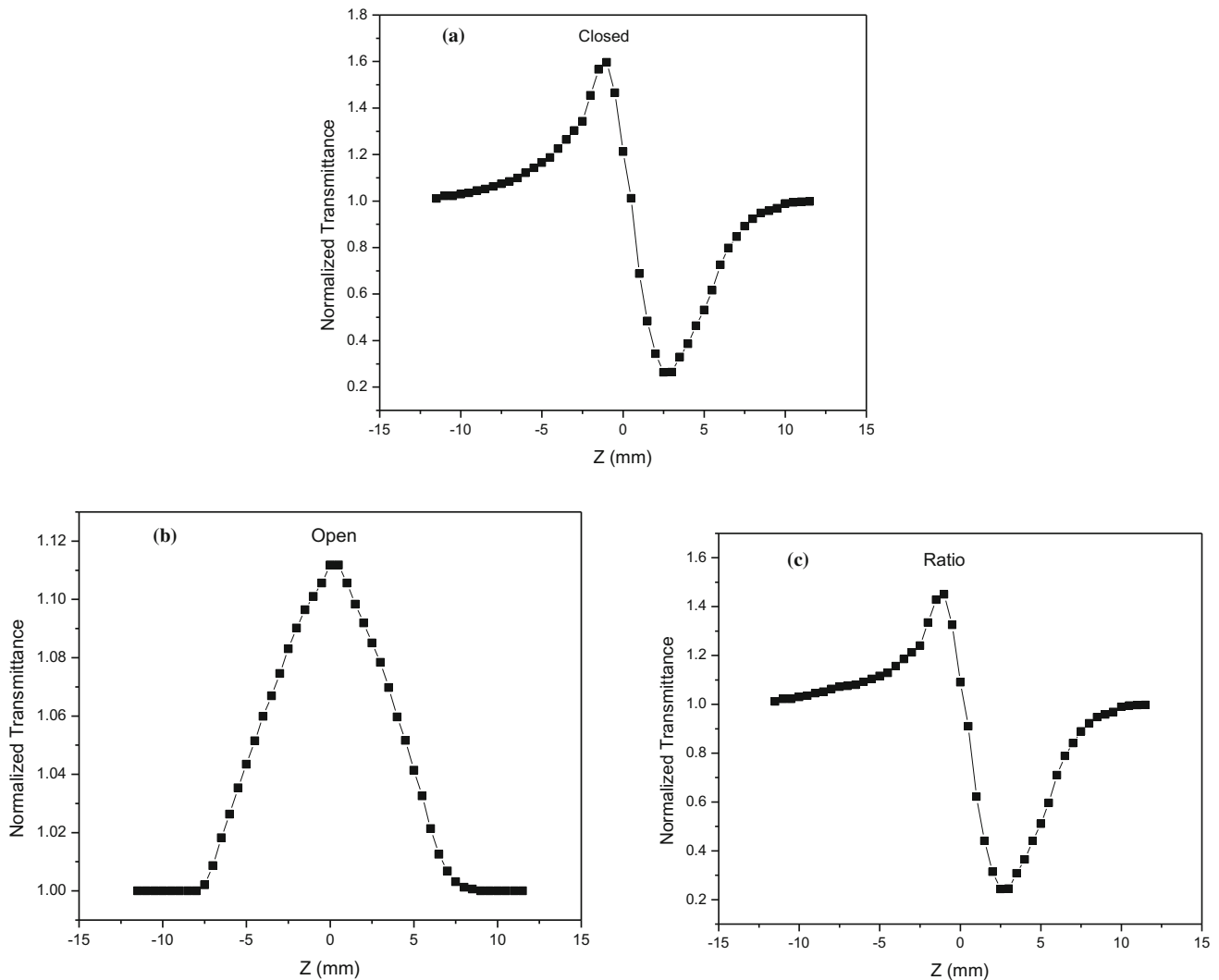


**Fig. 13** **a** Closed aperture, **b** open aperture, **c** ratio of closed to open aperture Z-scan for grown 3,4-dimethoxybenzaldehyde-2,4-dinitroaniline

$$\Delta T_{p-v} = 0.406(1 - S)^{0.25} |\Delta\phi_0|$$

where  $\Delta\phi_0$  is the on-axis phase shift at the focus and  $S$  is the aperture linear transmittance which is given by the equation

$$S = 1 - \exp(-2r_a^2/\omega_a^2)$$

where  $r_a$  denotes the aperture radius and  $\omega_a$  denotes the radius of the laser spot before the aperture. The on-axis phase shift is related to the third order nonlinear refractive index ( $n_2$ ) by,

$$|\Delta\phi_0| = kn_2L_{\text{eff}}I_0$$

where  $L_{\text{eff}} = (1 - e^{-\alpha L})/\alpha$ , with  $L$  the sample length,  $\alpha$  the linear absorption coefficient,  $I_0$  the intensity of the laser beam at focus  $z = 0$  and  $k$  the wave number

( $k = 2\pi/\lambda$ ). The nonlinear absorption coefficient  $\beta$  is estimated from the open aperture Z-scan mode data using the relation

$$\beta = \frac{2\sqrt{2} \cdot \Delta T}{I_0 \cdot L_{\text{eff}}}$$

where  $\Delta T$  is the maximum value of the open aperture normalized transmittance obtained from the Z-scan plot. Experimentally determined nonlinear refractive index  $n_2$  and nonlinear absorption coefficient  $\beta$  can be used to find the real and imaginary parts of the third-order nonlinear optical susceptibility [ $\chi^3$ ] according to the following relations

**Table 5** Nonlinear parameters of 3,4-dimethoxybenzaldehyde-2,4-dinitroaniline in acetone

Parameters	Measured values
Nonlinear refractive index ( $n_2$ )	$5.56 \times 10^{-8}$ cm <sup>2</sup> /W
Nonlinear absorption coefficient ( $\beta$ )	$0.07 \times 10^{-4}$ cm/W
Real part of third order susceptibility [ $\text{Re}(\chi^3)$ ]	$2.11 \times 10^{-6}$ esu
Imaginary part of third order susceptibility [ $I_m(\chi^3)$ ]	$0.45 \times 10^{-6}$ esu
Third order nonlinear susceptibility ( $\chi^3$ )	$2.16 \times 10^{-6}$ esu

$$\text{Re}\chi^3(\text{esu}) = \frac{10^{-4}(\varepsilon_0 c^2 n_0^2 n_2)}{\pi} \quad (\text{cm}^2/\text{W})$$

$$I_m\chi^3(\text{esu}) = \frac{10^{-2}(\varepsilon_0 c^2 n_0^2 \lambda \beta)}{4\pi^2} \quad (\text{cm}/\text{W})$$

where  $\varepsilon_0$  is the vacuum permittivity, and  $c$  is the light velocity in vacuum. The absolute value of the third-order nonlinear optical susceptibility is given by the relation

$$|\chi^3| = \left[ (\text{Re}(\chi^3))^2 + (I_m(\chi^3))^2 \right]^{1/2}$$

The nonlinear parameters are calculated and the obtained values are tabulated in Table 5.

## 4 Conclusion

The organic material 3,4-dimethoxybenzaldehyde-2,4-dinitroaniline single crystal was successfully grown by slow evaporation technique using acetone as solvent. The single crystal XRD studies show that the grown crystal belongs to the monoclinic crystal system with the centro-symmetric space group  $P2_1/n$ . The powder XRD reveals that the grown crystal has good crystalline nature. The FTIR and the FT-Raman spectral analyses confirmed the presence of various functional groups in the 3,4-dimethoxybenzaldehyde-2,4-dinitroaniline single crystal. The optical (UV–Vis–NIR) analysis reveals that the crystal have good transmission in the entire visible and near infrared regions. The optical band gap of the grown crystal was found to be 3.9 eV using Tauc plot. The linear optical parameters such as refractive index, extinction coefficient and optical conductivity were calculated for the grown crystal. The Urbach energy was calculated as 0.3 eV which indicates the crystalline perfection of the grown crystal. The photoluminescence analysis shows that the high intensity peak was obtained around 530 nm, and it shows green colour emission. Thermal properties indicate that the obtained single crystal melting point is

almost nearly 90 °C and the decomposition point is around 279 °C. The kinetic parameters for the thermal decomposition of the grown crystal were calculated using Coats–Redfern method. The dielectric analyses reveal that the dielectric constant, the dielectric loss and the AC conductivity were gradually increases with the increase of temperature and it may be realized as due to the temperature variations of the polarizability. The value of activation energy is found to be 0.139 eV. The electronic properties such as the plasma energy, the Penn gap, the Fermi energy and the electronic polarizability are calculated. The third-order nonlinear analysis reveals that the organic 3,4-dimethoxybenzaldehyde-2,4-dinitroaniline single crystal exhibits negative optical nonlinearity.

## Acknowledgements

This work was supported by the University Grants Commission (UGC), South Eastern Regional Office (SERO), Government of India, under the grant of Minor Research Project UGC Reference No: F. MRP-7005/16 (SERO/UGC) Link No: 7005, is hereby gratefully acknowledged.

## References

1. P.A. Franken, A. Hill, C.W. Peters, G. Weinrich, *Phys. Rev. Lett.* **7**, 118–119 (1961)
2. S.R. Marder, J.E. Sohn, G.D. Stucky, *Materials for Nonlinear Optics* (American Chemical Society, Washington, 1991).
3. S. Suresh, A. Ramanand, D. Jayaraman, P. Mani, *Rev. Adv. Mater. Sci.* **30**, 175–183 (2012)
4. D. JanardhanaRao, B. Hari Babu, A.V.V.S. Swami, S. Sumithra, *Univ. J. Environ. Res. Technol.* **3**, 225–232 (2013)
5. M. Somac, A. Somac, B.L. Davies, M.G. Humphery, M.S. Wong, *Opt. Mater.* **21**, 485–488 (2002)
6. J.G. Breitzar, D.D. Diott, L.K. Iwaki, S.M. Kirkpatrick, T.B. Rauchturs, *J. Phys. Chem. A* **103**, 6930–6937 (1999)

7. R.K. Choubey, R. Trivedi, M. Das, P.K. Sen, P. Sen, S. Kar, K.S. Bartwal, R.A. Ganeev, *J. Cryst. Growth* **311**, 2597–2601 (2009)
8. R.K. Choubey, S. Medhekar, R. Kumar, S. Mukherjee, S. Kumar, *J. Mater. Sci. Mater. Electron.* **25**, 1410–1415 (2014)
9. B.K. Dadhich, I. Kumar, R.K. Choubey, B. Bhushan, A. Priyam, *Photochem. Photobiol. Sci.* **16**, 1556–1562 (2017)
10. R.P. Jebin, T. Suthan, CCDC 1569865: Experimental Crystal Structure Determination (2017). <https://doi.org/10.5517/ccdc.csd.cclppktr>
11. J. Ramajothi, S. Dhaanuskodi, *Spectrochim. Acta Part A* **68**, 1213–1219 (2007)
12. C.N. Banwell, E.M. McCash, *Fundamentals of Molecular Spectroscopy*, 4th edn. (Tata McGraw-Hill, New Delhi, 1994).
13. F. Moser, F. Urbach, *Phys. Rev.* **102**, 1519–1523 (1956)
14. B.K. Periyasamy, R.S. Jebas, N. Gopalakrishnan, T. Balasubramanian, *Mater. Lett.* **61**, 4246–4249 (2007)
15. P. Karuppusamy, M.S. Pandian, P. Ramasamy, S. Verma, *Opt. Mater.* **79**, 152–171 (2018)
16. T. Suthan, N.P. Rajesh, *J. Cryst. Growth* **312**, 3156–3160 (2010)
17. T. Suthan, P.V. Dhanaraj, N.P. Rajesh, *Spectrochim. Acta Part A* **87**, 194–198 (2012)
18. R.P. Jebin, T. Suthan, N.P. Rajesh, G. Vinitha, U. Madhusoodhanan, *Spectrochim. Acta Part A* **135**, 959–964 (2015)
19. M. Saravanan, S.A. Rajasekar, *Opt. Mater.* **54**, 217–228 (2016)
20. M.A. Ashok, B.N. Achar, *Bull. Mater. Sci.* **31**, 29–35 (2008)
21. S. Rama, C.S. Dilip, R.N. Perumal, *J. Cryst. Growth* **409**, 32–38 (2015)
22. V. Gupta, K.K. Bamzai, P.N. Kotru, B.M. Wanklyn, *Mater. Sci. Eng. B* **130**, 163–172 (2006)
23. V. Hangloo, K.K. Bamzai, P.N. Kotru, M.L. Koul, *Bull. Mater. Sci.* **27**, 395–401 (2004)
24. K. Gayathri, P. Krishnan, P.R. Raj Kumar, G. Anbalagan, *Bull. Mater. Sci.* **37**, 1589–1595 (2014)
25. T. Suthan, N.P. Rajesh, P.V. Dhanaraj, C.K. Mahadevan, *Spectrochim. Acta Part A* **75**, 69–73 (2010)
26. T. Suthan, P.V. Dhanaraj, N.P. Rajesh, C.K. Mahadevan, G. Bhagavannarayana, *Cryst. Eng. Comm.* **13**, 4018–4024 (2011)
27. T. Akutagawa, S. Takeda, T. Hasegawa, T. Nakamura, *J. Am. Chem. Soc.* **126**, 291–294 (2004)
28. T. Arumanayagam, P. Murugakoothan, *J. Miner. Met. Mater. Eng.* **10**, 1225–1231 (2011)
29. T. Suthan, N.P. Rajesh, C.K. Mahadevan, G. Bhagavannarayana, *Mater. Chem. Phys.* **129**, 433–438 (2011)
30. S. Karuppusamy, K. Dinesh Babu, V. Nirmal Kumar, R. Gopalakrishnan, *Appl. Phys. A* **122**, 498 (2016)
31. S. Siva Bala Solanki, N.P. Rajesh, T. Suthan, *Opt. Laser Technol.* **103**, 163–169 (2018)
32. P.B. Chapple, J. Staromlynska, J.A. Hermann, T.J. Mckay, *J. Nonlinear Opt. Phys. Mater.* **6**, 251–293 (1997)
33. S. Suresh, M.N. Mohideen, G. Vinitha, R.M. Kumar, *Mod. Electron. Mater.* **4**, 103–111 (2018)
34. T. Cassano, R. Tommasi, M. Ferrara, F. Babudri, G.M. Fari-nola, F. Naso, *Chem. Phys.* **272**, 111–118 (2001)

**Publisher's Note** Springer Nature remains neutral with regard to jurisdictional claims in published maps and institutional affiliations.